A Combined Resource Allocation Framework for PEVs Charging Stations, Renewable Energy Resources and Distributed Energy Storage Systems

S. M. Kandil[a], Hany E.Z. Farag[a,*], Mostafa F. Shaaban[b], M. Zaki El-Sharafy[a]

[a]Department of Electrical Engineering and Computer Science, York University, 4700 Keele Street, Toronto, ON, Canada M3J 1P3

[b]Department of Electrical Engineering, American University of Sharjah, University City, Sharjah, UAE

* Corresponding author. Tel.: +1 (416) 736-2100 ext. 33844; Email address: hefarag@cse.yorku.ca

Abstract

The massive deployment of plug-in electric vehicles (PEVs), renewable energy resources (RES), and distributed energy storage systems (DESS) has gained significant interest under the smart grid vision. However, their special features and operational characteristics have created a paradigm shift in distribution network resource allocation studies. This paper presents a combined model formulation for optimal resource allocation of PEVs charging stations, RES and DESS in distribution networks. The formulation employs a general objective function that optimizes the total Annual Cost of Energy (ACOE). The decision variables in the formulation are the locations and capacities of PEVs charging stations, RES, and DESS units. Also, the formulation accounts for the uncertainties of PEVs charging demand and output generation of RES units. The formulation is decomposed into two interdependent sub-problems and solved using a combination of metaheuristic and deterministic optimization techniques. A sample case study is presented to illustrate the performance of the algorithm.

Keywords— Charging stations, Distribution system resource allocation, Electric vehicles, Energy storage systems, Genetic algorithms, Monte Carlo simulation, and Renewable energy

NOMENCLATURE

d, h	Index of days and hours	i, j	Index of buses
s, v	Index of scenarios and PEV respectively	$A_{(d,h,s)}$	Arrival rates in *vehicle/h*
$a_{EV(i)}$	Binary decision variables indicating the decision of installing charging stations at bus i	$a_{RE(i)}, a_{ES(i)}$	Binary decision variables for the installation of RES and DESS at bus i, respectively
$\mathscr{b}_{EV(i)}$	Integer decision variable indicating the number of charging stations installed at bus i	$\mathscr{b}_{RE(i)}$	Integer decision variable indicating the size of RES at bus i

https://doi.org/10.1016/j.energy.2017.11.005

$\mathscr{b}_{ES1(i)}\mathscr{b}_{ES2(i)}$	Integer decision variables indicating the size of DESS in *kW* and *kWh* respectively	C_{CH}	Capital cost of PEV charger installations in *$/charger*
C_{Loss}, C_{cons}	Costs of energy losses and energy consumed by PEVs, normal load, and DESS	C_{RE}^{kw}	Capital cost of RE installations in *$/kW*
C_{EV}, C_{RE}, C_{ES}	Capital and operating costs for PEV chargers, RES units and DESS, respectively	C_{ES}^{OM}	Operation and maintenance cost of DESS in *$/kWh*
$C_{ES}^{kwh}, C_{ES}^{kw}$	Capital cost of DESS installations in *$/kWh* and *$/kW*	$CDF_{A(d,h)}^{-1}$	Inverse of the cdf describing the arrival rates
$CDF_{T(d,h)}^{-1}$	Inverse of the cdf of the parking duration	$E_{BAT(i,d,s,v)}$	Rated *kWh* for the battery of vehicle *v*
$E_{D(i,d,s,v)}$	The delivered energy in *kWh* to vehicle v	$E_{ES(i,d,h,s)}$	Stored energy in DESS at each hour *h*
E_{ES}^{Cap}	Capacity of DESS in *kWh*	E_{ES}^{step}	Defined step of DESS sizing in *kWh*
$E_{REQ(i,d,s,v)}$	Required *kWh* by vehicle *v*	$f_{(i,d,h,s,v)}^{CH}$	Relation between P_{PEV}^{Max} and the SOC level
$f(O_k, \Theta)$	Probability function of random sample O_k	$\vec{I}_{(i,j)}, I_{(i,j)}$	Phasor and magnitude of current flow between buses i, j
$I_{(i,j,d)}^{Max}$	Capacity of the line between buses i, j in day d	LT, LV	Life time of equipment and the levelized cost factor
$N_{A(d)}^{days}$	Number of actual days that are represented by each day *d*	N_s	Number of virtual scenarios
$N_{VH(h)}$	Total number of arrived vehicles for hour h	$Pro_{(s)}$	Probability of occurrence of scenario s
$p_{RE}^{MCS}, pf_{RE}^{Min}$	Per unit power and minimum power factor of RES	$P_{CH(v)}$	Actual charging power in *kW* of PEV v
P_{CH}^{Max}	Rated power of single PEV charger in *kW*	P_{RE}	Active power in *kW* delivered by RES
P_{EV}, P_{ES}	Active power in *kW* consumed by PEV, and DESS, respectively	$P_{EV}^{Cap}, P_{RE}^{Cap}, P_{ES}^{Cap}$	Total capacity in *kW* of installed PEV chargers, RES and DESS respectively
P_{Grid}, Q_{Grid}	Generated active and reactive powers from grid in *kW*	P_{inj}, Q_{inj}	Injected active and reactive powers at each bus in *p.u.*
P_{Rev}^{Max}	Allowable limits of reverse active power flow	P_{NL}, Q_{NL}	Normal active and reactive powers at each hour *h* in *kW*
$P_{PEV(v)}^{Max}$	Maximum allowable charging rate in *kW* for PEV v	$P_{RE}^{Step}, P_{ES}^{Step}$	Defined step of RES and DESS sizing in *kW*
Q_{ES}^{Max}	Available reactive power at each hour *h*	Q_{RE}, Q_{ES}	Reactive power settings at each hour *h*
r, f	Interest and inflation rates	R_{RE}	The return of selling energy from RES in *$*
r_s, α, β	Solar irradiance and parameters of solar pdf	S_{base}	Base power in *kVA*
$SOC_{ES(i)}^{Min}$	Minimum allowed SOC of the DESS	$SOC_{(i,d,h,s,v)}$	The PEV battery SOC in %
$T_{(d,h,v)}$*	Parking duration in *h* for vehicle v	$U_{(s)}$	Uniformly distributed random number from 0 to 1
$\vec{V}_{(i)}, V_{(i)}, \delta_{(i)}$	Phasor, magnitude in *p.u.* and angle of voltage at each bus *i*	V^{Min}, V^{Max}	Minimum and maximum allowed voltage limits
ws, c	Wind speed and scale index, respectively	X_{ES}^{P}, X_{ES}^{Q}	Decision variable for DESS active and reactive powers control.
X_{EV}	Decision variable for PEV charging	X_{RE}^{P}, X_{RE}^{Q}	Decision variable for RES active and reactive powers control.
$\vec{Y}_{(i,j)}, Y_{(i,j)}, \theta_{(i,j)}$	Phasor, magnitude and angle of Y-bus matrix	$\mathcal{I}_{EV}, \mathcal{I}_{RE}$	Sets of candidate buses for PEVs and RES
$\mathcal{I}_{ES}$	Candidate buses for DESS	$\eta_{CH,}\ \eta_{ES}$	Efficiency of PEV chargers and DESS units
$\rho_{RE(h,d,s)}^{kwh}$	Price of selling RES energy in *$/kWh*	$\rho_{Grid(h,d,s)}^{kwh}$	Price of energy delivered from the grid in *$/kWh*
Ω_1	Set of installation variables	Ω_2	Set of operation variables

1. INTRODUCTION

Reducing greenhouse gas emissions have gained global interest over the last few decades. A key factor for reducing these emissions is shifting towards renewable energy resources (RESs) in electricity generation and low or zero emission vehicles in transportation. Electrification of the transportation sector is currently the most viable option for reducing transportation emissions and thus the production of plug-in electric vehicles (PEVs) is predicted to rise dramatically in the next few decades [1]. Current distribution system structure is capable of accommodating low penetration levels of uncontrolled PEV charging (i.e. charging starts as soon as PEVs are plugged). However, looking to the future, the increasing use of PEVs will have a considerable impact on the demand for electricity and the development of future power grids. Recent studies showed that the rapid growth of PEVs along with the additional energy consumption likely to cause severe consequences on the existing grid [2]–[4]. Hence, the deployment of high PEV penetration in distribution networks will require: 1) upgrading current system infrastructure so that it can accommodate uncoordinated charging, and/or 2) integration of smart grid solutions to coordinate PEV charging via real-time monitoring and control (i.e. optimal scheduling of PEVs charging, where the battery pack of PEV acts as a controllable load) [5].

Yet, supplying the extra load imposed by charging PEVs from conventional electricity generation resources will shift the emissions from the transportation sector to the electricity generation sector. To allay this concern, RESs are expected to play an important role in powering the transportation sector [6], [7]. Levels of RESs penetration have been rising satisfactorily due to government incentives and developing technology in this area. However, integrating large levels of RES into the grids is also challenging as the variable and unpredictable nature of wind and solar exposes the grid to stability issues and makes the investment planning of future power grids more complicated [8].

Despite these challenges, other considerations show promise. Distributed energy storage systems (DESS) can be a critical component of grid stability and resiliency [9]. The grid integration of DESS technologies would reduce the intermittency of RES, thus increasing their capacity factor [10]. DESS can also prevent wastage of excess renewable energy feeding into the grid at times when production is at a peak, but demand is

low by effectively storing this energy [10], [11]. In addition, integrating DESS into existing grids could enable confident supply deployment of PEVs by ensuring a stable and consistent supply of the electricity vital to charge their batteries [12].

The combined integration of PEVs, RES, and DESS technologies has been recently gained interest in industry [13]–[15]. This, in turn, introduces a paradigm shift in utility studies of power distribution systems. Due to the interesting and recent subject, numerous efforts have been spent on related research. Yet, most of the literature work in the area of PEV charging in combination with RES and/or DESS is focused on the operational aspects and optimal coordination in real-time [16], [17], while few researchers have proposed methods to address the resource allocation perspectives. Without consideration of RES and DESS, the authors in [18] proposed a method for optimal allocation of residential and commercial parking lots in a distribution network. An algorithm is developed in [19] to determine the optimum locations and sizes of PEV charging stations in a distribution network with already installed RES. The authors in [20] introduced a method to mitigate the impacts of PEV charging by allocating dispatchable distributed generation (DG) units in distribution networks. However, the work in [20] didn't include consideration of RES and DESS. Further, the locations and sizes of PEVs charging stations in [20] have been assumed to be predetermined. In [21], a multi-objective long term resource allocation algorithm has been proposed to accommodate high penetration of PEV and RES. However, the work in [21] did not take DESS into account. Moreover, all previous works in [18]–[21], ignored the impacts of the optimal operation scheduling, such as 1) coordinated PEV charging, 2) smart inverter control of RES units, and 3) smart scheduling of DESS, in the resource allocation process. Optimal operational scheduling of these technologies reduces their negative impact on existing distribution networks and increases their penetration levels. In consequence, optimal operation scheduling will affect the optimal location and sizing of PEVs, RES, and DESS significantly and it has to be taken into account in the resource allocation studies. Recently, the authors in [22]–[24] presented integrated approaches for distribution system planning studies considering PEVs, RES and DESS. However, the approaches in [22]-[24] were tailored particularly for reliability studies.

Based on these considerations, this paper presents a model formulation for optimal locations and capacities of grid-interfaced PEV chargers in parking lots in conjunction with RES and DESS in distribution networks. The objective of the formulated problem is to minimize the overall capital and operational Annual Costs of Energy (ACOE). The central features that differentiate this work from the previous literature are: 1) it is comprehensive; where it simultaneously integrates the optimal installations of PEVs charging stations, RES units, and DESS in a combined framework. 2) The formulation accounts for the uncertainty accompanied with PEV charging demand in parking lots. In this regard, practical historical data of conventional vehicles in commercial and residential parking lots has been utilized to develop a scenario-based algorithm for modeling the PEVs charging demand. 3) The coordinated operation scheduling of PEVs charging, output active and reactive power control of RES units, and DESS charging/discharging settings, for the generated scenarios, has been integrated into the proposed formulation to account for their impacts on the solution of the resource allocation problem. 4) A stochastic Mixed-Integer Nonlinear programming (MINLP) problem has been formulated for the combined resource allocation framework. In order to be solved, the problem has been decomposed into two interdependent sub-problems: exterior and interior. As depicted in Fig.1, the exterior sub-problem represents the installation problem and it contains the solution space of the number, location and capacities of PEVs charging, and RES, and DESS output power for each candidate solution in the exterior sub-problem. A combination of metaheuristic and deterministic optimization techniques has been utilized to solve the exterior and interior sub-problems concurrently.

The remainder of this paper is organized as follows: Section 3 introduces the modeling of the smart distribution system components. Sections 4, and 5 present the problem formulation and its proposed solution mechanism. Several case studies, simulation results, and corresponding discussions are presented in Section 6. Section 7 concludes the paper and summarizes its main contribution.

2. MODELING OF PEVS, RES, AND DESS

Characteristics of components such as the uncertain nature of PEVs charging demand and RES output power generation should be modeled properly in the resource allocation studies of smart distribution grids. In this section, the required modeling of the power demand and generation components (i.e. PEV demand, normal load, RES, and DESS) is discussed. To that end, a unified scenario-based approach is considered in this work, where the models for all components are developed based on the assumption that the entire year is divided into four seasons, and two days are representing each season: weekday and weekend. Further, each day is divided into 24-hour time segment, where each hour has its own probability distribution functions (pdfs) for the PEVs charging demand and the output power of RES units. A description of the model of each component is presented hereunder.

2.1 PEV Demand Modeling:

There are two major variables that affect the PEV load model in a charging station: arrival rate and parking durations. Since, each type of parking lots (e.g. residential, commercial downtown, commercial commute) has unique arrival rates and parking durations, a generalized model is proposed in this work, which utilizes Monte Carlo Simulation (MCS) to generate virtual scenarios for PEV arrivals and parking durations. The proposed model utilizes practical historical data of arrival rates and parking durations of conventional vehicles in several parking lots in Toronto, Ontario, Canada. These data are made available through Toronto Parking Authority. Fig.2 shows a flowchart of the proposed PEV arrival rate model. As shown in the Figure, the historical hourly data of PEVs arrivals and parking durations of each type of parking lots is clustered into seasons. The data of each season is clustered into weekdays and weekends i.e.,

the entire year is modeled by eight days: 4 seasons $\times 2$ days. Hence, the arrival rates in each of the 24 hours of the eight days representing the year are extracted from the historical data. Using the Maximum Likelihood Estimation (MLE) approach, different types of pdfs are used to fit the arrival data for each hour *h*. Let us suppose we have a random sample of arrival rates $O_1, O_2, ..., O_n$ whose assumed probability distribution

depends on some unknown parameter Θ. The primary goal of MLE is to find a point estimator $u(O_1, O_2, ..., O_n)$, such that $u(o_1, o_2, ..., o_n)$ is a good point estimate of Θ, where $o_1, o_2, ..., o_n$ are the observed values of the random sample. For example, if it is planned to take a random $O_1, O_2, ..., O_n$ for which the O_i are assumed to be normally distributed with mean μ and variance σ^2, then the goal is to find a good estimate of μ, using the data $o_1, o_2, ..., o_n$ obtained from the specific random sample. A good estimate of the unknown parameter Θ would be the value of Θ that maximizes the likelihood of getting the observed data. Given the probability function $f(o_k, \Theta)$ of each random sample O_k, the joint pdf of $O_1, O_2, ..., O_n$ can be formulated as follows:

$$pdf_{(h,d)}(\Theta) = prob(O_1 = o_1, O_2 = o_2, ..., O_n = o_n) = \prod_{k=1}^{n} f(o_k, \Theta) \qquad (1).$$

Therefore, for each of the eight days representing the entire year, there are 48 parameters ($24\text{h} \times 2$ parameters, i.e. mean μ and variance σ^2), calculated from the historical data of the arrival rates. For each hour *h* in day *d*, the inverse of the cumulative distribution function (CDF) is calculated and used to generate N_S virtual scenarios of PEV arrivals given as:

$$A_{(d,h,s)} = CDF^{-1}_{A(d,h)}\left(U_{(s)}\right) \qquad \forall d, h, s \leq N_s \qquad (2).$$

Afterwards, the virtual parking durations are generated for all arrived vehicles in all scenarios for hour *h* in day *d*, as follows:

$$T_{(d,h,s)} = CDF^{-1}_{T(d,h)}\left(U_{(v)}\right) \qquad \forall d, h, s \leq N_{VH(h)} \qquad (3).$$

As given in (2) and (3), the scenarios of both arrival rates and parking durations are generated according to their individual *CDF*s at each hour *h* of day *d*. It is noteworthy that the time index correlates the generated scenarios of arrival rates and parking durations. Further, it is assumed in this work that the generated virtual scenarios at each hour *h* are independent on their preceding generated scenarios at *h-1*. Also, due to lack of PEVs charging data, the arriving PEVs in each hour *h* for the different scenarios are assigned random values

of required charging energy E_{REQ} and charging rate limit P_{CH} according to a standard uniform distribution. The assigned values are bounded between minimum and maximum values, which are chosen based on the available PEVs in the market [1]. Hence for each scenario *s*, the parking duration *T* and the required charging energy E_{REQ} and charging rate P_{CH} are defined for each vehicle *v* arrives to the parking lot at hour *h* of day *d*. The output of the PEV model can be regarded as virtual scenarios of PEVs charging, which are further quantified into power demand from the grid in the developed formulation.

A sample of ten virtual scenarios in March for a public downtown garage parking with a capacity of 100 parking spots is presented in Fig.3. Scenarios 1 to 5 represent the PEV profiles for a weekend, while the rest of scenarios represent a weekday. As shown in the figure, the arrival rates during the weekdays are much higher than those in the weekends. Here it is worth noting that the total consumed power of PEVs, at each hour *h* in day *d* and scenario *s*, is governed by the number of available charging stations and the charging scheduling as will be illustrated in the problem formulation given in the next section.

2.2 RES Generated Output Power Modeling:

The output power of intermittent RES should be appropriately modeled in the resource allocation studies. For PV systems, the output power of modules depends on the amount of solar irradiance, ambient temperature and characteristics of the module itself. For this research, the solar irradiance for each hour *h* of day *d* is modeled by the Beta pdf using historical data [21] given as follows:

$$f_b(r) = \frac{\Gamma(\alpha+\beta)}{\Gamma(\alpha)\Gamma(\beta)} \times r_s^{(\alpha-1)} \times (1-r_s)^{(\beta-1)} \qquad 0 \le r_s \le 1, \alpha \ge 0, \beta \ge 0 \qquad (4).$$

Using the Beta pdf parameters, a MCS is used to generate a number of virtual scenarios, which mimic the history for the solar irradiance (i.e. same as described in the PEVs model). The simulated values of solar irradiance and average monthly temperatures are then converted into output power based on the characteristics of the PV panels as discussed in [21].

Similar to PV, the output power of wind turbines depends on the wind speed and parameters of the speed-power conversion curve. In order to get the pdf of wind speed and parameters of the speed-power conversion

curve, again, two days can be selected as representatives of each season. Each day is further divided into 24-hour time segments, each having a pdf for the wind speed. Once the wind speed is modeled for each hour, the probabilistic function of the output power of wind turbines can be easily generated. The wind speed is usually modeled using the Rayleigh pdf which is a special case of the Weibull pdf given as [21]:

$$f_w(ws) = \left(\frac{2ws}{c^2}\right) \times \exp\left[-\left(\frac{ws}{c}\right)^2\right] \quad (5).$$

It is noteworthy that *c* equals approximately 1.128 of the mean wind speed, where the mean value of wind speeds is calculated using the historical data of each time segment. The output power of the wind turbine is then calculated using the turbine characteristics.

2.3 DESS Modeling:

In this work, the DESS inverter is represented by the four quadrants model, as shown in Fig.4, for any type of DESS, such as Li-ion, Lead-acid, and Ni-cadmium batteries. DESS is modeled as a load during charging periods and as a generator during discharging periods. At each time step, the DESS receives two reference signals for active and reactive powers, which represent the decision variables of the optimal operating schedule of the DESS. The reference signals are different in the operation time horizon (i.e. from one hour to another) based on the system state. Technical limitations on the stored energy, SOC level, charge/discharge rates, and reactive power limits are incorporated into the problem formulation described in Section 4.

2.4 Normal Load Modeling:

The normal load model is assumed to follow the reliability test systems (RTS) Load pattern [21], where uncertainty of -5% to +5% is added as a uniform distribution to generate random scenarios of normal load for each hour *h* of day *d*.

3. Problem Formulation

This section presents the mathematical formulation of the combined resource allocation framework. The objective function is based on the total ACOE, which is calculated from the summation of 1) discounted

investment costs of installing the new technologies (PEVs, RES, and DESS), 2) discounted cost of energy consumption and losses, and 3) discounted revenue of RES power production. It is assumed that the total ACOE does not include financing issues, future replacement, or degradation costs. Each of these can be included for thorough analysis. The objective function is represented as follows:

$$\min_{\Omega_1,\Omega_2} \sum_s Pro(s) \times \left(\sum_i \left[C_{RE(i)} - R_{RE(i,s)} + C_{ES(i)} + C_{EV(i,s)}\right] + \left[C_{loss(s)} + C_{cons(s)}\right]\right) \quad (6)$$

where,

$$C_{RE(i)} = C_{RE(i)}^{kw} \times P_{RE(i)}^{Cap} / LV \quad (7)$$

$$R_{RE(i,s)} = \sum_d N_{A(d)}^{days} \sum_h \rho_{RE(i,h,d,s)}^{kwh} \times P_{RE(i,h,d,s)} \quad (8)$$

$$C_{ES(i,s)} = \left(C_{ES(i)}^{kw} P_{ES(i)}^{Cap} + C_{ES(i)}^{kwh} E_{ES(i)}^{Cap}\right) / LV + C_{ES(i)}^{OM} \quad (9)$$

$$C_{EV(i,s)} = C_{CH}\, \mathscr{b}_{EV(i)} / LV \quad (10)$$

$$[C_{Loss(s)} + C_{cons(s)}] = \sum_i \left(\sum_d \left(N_{A(d)}^{days} \sum_h \rho_{Grid(i,h,d,s)}^{kwh} \times P_{Grid(i,h,d,s)} \right) \right) \quad (11)$$

$$LV = \frac{(1+r')^{LT} - 1}{r'(1+r')^{LT}} \qquad \& \qquad r' = \frac{r - f}{1 + f} \quad (12).$$

As shown in (6), the various decision variables that influence the objective function can be classified into two interdependent sets: Ω_1 and Ω_2. The set Ω_1 contains the *installation variables* that represent the locations, numbers, and capacities of PEVs, RESs and DESS units, i.e. $\Omega_1 = \{a_{EV}, \mathscr{b}_{EV}, a_{RE}, \mathscr{b}_{RE}, a_{ES}, \mathscr{b}_{ES1}, \mathscr{b}_{ES2}\}$. On the other hand, the set Ω_2 contains the *operation scheduling variables* of PEVS charging and RES/DESS output active and reactive powers for each hour *h* of day *d* and scenario *s* i.e. $\Omega_2 = \{X_{EV}, X_{RE}^P, X_{RE}^Q, X_{ES}^P, X_{ES}^Q\}$. The objective function is thus subject to two categories of constraints: installation and operation. A description of these constrains is presented here under.

3.1 Installation Constraints:

For each location *i* that is not candidate for installations of PEVs charging stations, RES units and DESS, the installation variables are set to zeros as follows:

$$a_{EV(i)}, \mathscr{b}_{EV(i)} = 0 \quad \forall i \notin \mathcal{I}_{EV} \tag{13}$$

$$a_{ES(i)}, \mathscr{b}_{ES1(i)}, \mathscr{b}_{ES2(i)} = 0 \quad \forall i \notin \mathcal{I}_{ES} \tag{14}$$

$$a_{RE(i)}, \mathscr{b}_{RE(i)} = 0 \quad \forall i \notin \mathcal{I}_{RE} \tag{15}.$$

The capacities of the PEVs charging stations, RES and DESS at each location *i* are governed by the manufacturer rating of the PEV chargers and the step of power sizing for RES and DESS, respectively given as:

$$P_{EV(i)}^{Cap} = a_{EV(i)} \times \mathscr{b}_{EV(i)} P_{CH(i)}^{Cap} \tag{16}$$

$$P_{RE(i)}^{Cap} = a_{RE(i)} \times \mathscr{b}_{RE(i)} \times P_{RE(i)}^{Step} \tag{17}$$

$$P_{ES(i)}^{Cap} = a_{ES(i)} \times \mathscr{b}_{ES1(i)} \times P_{ES(i)}^{Step} \tag{18}$$

$$E_{ES(i)}^{Cap} = a_{ES(i)} \times \mathscr{b}_{ES2(i)} \times E_{ES(i)}^{Step} \tag{19}.$$

It is worth noting that the capacities of the power electronic interfaces (i.e. inverters) in KVA of these technologies are assumed to be equal their active power capacities in KW.

3.2 Operation Constraints of PEVs Charging:

Based on the number of charging stations in each location *i*, i.e. $\mathscr{b}_{EV(i)}$, the total consumed power of PEVs at each hour *h* in day *d* and scenario *s* can be expressed in terms of the binary charging decision variable($X_{EV(i,d,h,s,v)}$) as follows:

$$P_{EV(i,d,h,s,v)} = \sum_{v} \frac{X_{EV(i,d,h,s,v)} \times P_{CH(i,d,h,s,v)}}{\eta_{CH(i)}} \quad , \quad X_{EV} \in \{0,1\} \tag{20}$$

where, the charging rate limits can be obtained as follows:

$$P_{CH(i,d,h,s,v)} = \begin{cases} P_{PEV(i,d,h,s,v)}^{Max} & \forall P_{PEV(i,d,h,s,v)}^{Max} \le P_{CH(i)}^{Max} \\ P_{CH(i,d,h,s,v)}^{Max} & \forall P_{PEV(i,d,h,s,v)}^{Max} > P_{CH(i)}^{Max} \end{cases} \tag{21}.$$

Also, the maximum allowable rate of charge for each vehicle v is formulated as a function of the SOC as in (22). The function f^{CH} describes the relation between the allowable maximum rate of charge and the SOC. For example, Li-ion batteries are usually charged in constant current mode (highest rate of charge) until the SOC

reaches high value; then, it is charged in constant voltage mode, which represents lower charging rate, to avoid excess battery charging [13, 20].

$$P^{Max}_{PEV(i,d,h,s,v)} = f^{CH}_{(i,d,h,s,v)} \times (SOC_{(i,d,h,s,v)}) \quad (22)$$

The total energy delivered for each vehicle *v* by the end of its parking duration must satisfy the customer requirements as follow:

$$E_{D(i,d,s,v)} = E_{BAT(i,d,s,v)} \sum_{h \in T_{(d,h,v)}} \frac{SOC_{(i,h,d,s,v)} - SOC_{(i,h-1,d,s,v)}}{100} \quad (23)$$

$$E_{D(i,d,s,v)} = E_{REQ(i,d,s,v)} \quad (24).$$

Further, the constraint in (25) relates the SOC of the battery of each vehicle *v* at time segment *h* to its SOC in the previous time segment as:

$$SOC_{(i,d,h,s,v)} = SOC_{(i,d,h-1,s,v)} + 100 \frac{X_{EV(i,d,h,s,v)} \times P^{Max}_{CH(i,d,h,s,v)}}{E_{BAT(i,d,s,v)}} \quad (25).$$

3.3 Operation Constraints of RES Active and Reactive Power:

Conventionally with low penetration level, RES units are uncontrolled and allowed to inject their maximum generated power to the grid. However, under the smart grid paradigm and with high RES penetration, a real-time active and reactive power control for RES inverters is expected. In such case, the inverter of RES unit receives a control signal from the distribution management system to indicate the percentage of active power curtailment and reactive power control with respect to the maximum generated power and the inverter capacity. Hence, each RES smart inverter to be located at bus $i \in \mathcal{I}_{RE}$ might receive two reference signals: $X^{P}_{RE(i)}$ and $X^{Q}_{RE(i)} \forall h, d, s$ to curtail its injected active power and control the reactive power given as follow:

$$P_{RE(i,d,h,s)} = (1 - X^{P}_{RE(i,h,d,s)}) \times p^{MCS}_{RE(h,d,s)} \times P^{Cap}_{RE(i)} \quad (26)$$

$$Q_{RE(i,h,d,s)} = X^{Q}_{RE(i,h,d,s)} \times P_{RE(i,h,d,s)} \times \tan[\cos^{-1}(pf^{Min}_{RE})] \quad (27)$$

$$\left|Q_{RE(i,h,d,s)}\right| \leq \sqrt{(P^{Cap}_{RE(i)})^2 - P^2_{RE(i,h,d,s)}} \quad (28)$$

$$0 \le X^{P}_{RE(i,h,d,s)} \le 1 \quad (29)$$

$$-1 \le X^{Q}_{RE(i,h,d,s)} \le 1 \quad (30).$$

3.4 Operation Constraints of DESS Active and Reactive Power:

Similar to RES, each DESS smart inverter to be located at bus $i \in \mathcal{I}_{ES}$might receive two reference signals: $X^{P}_{ES(i)}$and $X^{Q}_{ES(i)} \forall h, d, s$. The DESS stored energy at any time segment *h+1* is related to the stored energy in the previous time segment *h* as follows:

$$E_{ES(i,h+1,d,s)} = E_{ES(i,h,d,s)} + X^{P}_{ES(i,h,d,s)} \times P^{Cap}_{ES(i,h,d,s)} \quad (31).$$

The stored energy at time segment *h* is constrained by the maximum *kWh* capacity and the minimum allowed *SOC* of the DESS as follows:

$$\frac{SOC^{Min}_{ES(i)}}{100} \times E^{Cap}_{ES(i)} \le E_{ES(i,h,d,s)} \le E^{Cap}_{ES(i)} \quad (32).$$

Also, $P_{ES(i)}$ and $Q_{ES(i)} \forall h, d, s$ are dependent on the charging/discharging decision variables and constrained by the inverter capacity limits as follows:

$$P_{ES(i,h,d,s)} = X^{P}_{ES(i,h,d,s)} \times \frac{P^{Cap}_{ES(i,h,d,s)}}{\eta_{ES(i)}} \quad (33)$$

$$Q_{ES(i,h,d,s)} = X^{Q}_{ES(i,h,d,s)} \times Q^{Max}_{ES(i,h,d,s)} \quad (34)$$

$$(Q^{Max}_{ES(i,h,d,s)})^2 = (P^{Cap}_{ES(i)})^2 - P^2_{ES(i,h,d,s)} \quad (35)$$

$$-1 \le X^{P}_{ES(i,h,d,s)}, X^{Q}_{ES(i,h,d,s)} \le 1 \quad (36).$$

3.5 Operation Constraints of the Distribution System:

The objective function in (6) is subject to the equality constraints of the active and reactive power flow mismatch equations for each bus $i \, \forall h, d, s$ given as follows:

$$P_{inj(i,h,d,s)} = \sum_{j \in J} V_{(i,d,h,s)} V_{(j,h,d,s)} Y_{(i,j)} \times \cos(\theta_{(i,j)} + \delta_{(j,h,d,s)} - \delta_{(i,h,d,s)}) \quad (37)$$

$$Q_{inj(i,h,d,s)} = -\sum_{j \in J} V_{(i,h,d,s)} V_{(j,h,d,s)} Y_{(i,j)} \times \sin(\theta_{(i,j)} + \delta_{(j,h,d,s)} - \delta_{(i,h,d,s)}) \quad (38)$$

where,

$$P_{inj(i,h,d,s)} = \left(P_{RE(i,h,d,s)} + P_{ES(i,h,d,s)} - P_{EV(i,h,d,s)} - P_{NL(i,h,d,s)}\right) \times S_{base} \quad (39)$$

$$Q_{inj(i,h,d,s)} = \left(Q_{RE(i,h,d,s)} + Q_{ES(i,h,d,s)} - Q_{NL(i,h,d,s)}\right) \times S_{base} \quad (40).$$

The injected active and reactive powers from the main substation connected to the distribution system at bus $i=1$ can be represented as in (41) and (42). Also, the injected grid powers equal to the difference between the total consumption, represented by normal load, EV load, and losses, and the total local generation represented by RES and DESS.

$$P_{Grid(h,d,s)} = P_{inj(1,h,d,s)} \times S_{base} \quad (41)$$

$$Q_{Grid(h,d,s)} = Q_{inj(1,h,d,s)} \times S_{base} \quad (42)$$

It is also noted that due to technical issues, a reverse power flow limit might be applied at the main substation. Such limit is usually set as a percentage of the substation capacity. For instance, many LDCs in Canada limit the reverse power flow to a maximum of 60% of the substation capacity [21]. The reverse power flow constraint can be represented as:

$$\sum_{i \neq 1} P_{inj(i,h,d,s)} \leq P_{Rev}^{Max} \qquad \forall d, h, s \quad (43)$$

Also, the system voltage has to be kept within their specified maximum and minimum limits prescribed in the voltage regulation standards e.g. ANSI C84.1.

$$V^{Min} \leq V_{(i,h,d,s)} \leq V^{Max} \qquad \forall i, h, d, s \quad (44)$$

Similarly, the current flow in the distribution feeders is constrained by the thermal capability limit as follows:

$$I_{(i,j,h,d,s)} \leq I_{(i,j,d)}^{Max} \qquad \forall i, j, h, d, s \quad (45)$$

where, the phasor line current is calculated from the voltage state variables as follows

$$\vec{I}_{(i,j,h,d,s)} = \left(\vec{V}_{(j,h,d,s)} - \vec{V}_{(i,h,d,s)}\right)\vec{Y}_{(i,j)} \qquad \forall i, h, d, s \quad (46).$$

4. Problem Solution

The formulation described in the previous section is a mixed integer nonlinear programming MINLP problem. To lower its complexity, the problem is decomposed into two interdependent sub-problems i.e. exterior and interior. The exterior and interior sub-problems represent the installation and operational scheduling problems, which are controlled by the decision variable sets, Ω_1 and Ω_2, respectively. Fig.5 shows a flowchart that summarizes the proposed solution mechanism of the formulated resource allocation problem. As shown in the figure, a combination between metaheuristic technique and deterministic technique has been utilized to manage the exterior and interior parts concurrently. The GA toolbox under the Matlab® environment is used as the metaheuristic technique, which governs the exterior part by generating candidate solutions to the set of installation variables Ω_1 taking into account the specified installation constraints described in (13)-(19). As depicted in Fig.5, for each candidate solution Ω_1, an interior NLP optimization problem describing the operation scheduling is solved dynamically for each day *d* with a time step of one hour for each possible scenario *s* using GAMS. The NLP optimization problem includes the devices and system operation constraints described in (20)-(46). The objective is to recursively minimize the sum of daily operation costs for the eight days representing the entire year at the candidate installation variables provided from the GA solver. It is worth noting that the power flow equations described in (37)-(40) are defined in the NLP optimization model as equality constraints. Hence, the power flow equations does not require a designated solver, where the entire operation scheduling problem is solved using the built-in NLP GAMS solver. The solution of the interior part yields the set of decision variables for the operation scheduling, i.e. Ω_2 at each scenario *s* of hour *h* and day *d*. Then, based on Ω_1 and Ω_2, the total ACOE is calculated for each scenario. The fitness of each individual, i.e. Ω_1, is defined as the overall expected costs or the overall system annualized costs. The overall ACOE consists of the capital and operating costs of PEV charging stations, RES, and DESS and the cost of purchasing energy from the grid, which includes the energy losses and consumed energy. Based on the fitness of each individual in the population, the stopping criterion is checked. If the stopping criterion is met, the approach terminates

and the best individual is stored. If the stopping criterion does not met, the parents are selected through choosing elite child(s), crossover, and mutation. Then, a fitness proportionate selection is used to produce the new population of Ω_1.

5. Sample Case Study

The proposed resource allocation framework is tested using the 38-bus distribution system shown in Fig.6 [20]. The system contains a mix of residential, commercial and industrial customers being supplied from a common supply point. The total system peak load is 4.37 MVA. The interest rate and the inflation rate are assumed to be 5% and 1% respectively. The parameters for the PEV and the charging stations are represented in Table 1. The specification of the utilized PEV chargers is 208-240Volt AC, 7.2kW, 30Amp. It is noted that most of the expenses for the capital cost of home PEV chargers contribute to hardware, which are mainly in rural areas and are not considered in this work. On the other hand, for outdoor public PEV charging stations, installation cost is found to be dominant, which can be up to 80 % of the total costs [25]. The installation cost including labour, permits, and material, assumes that the installation site is not equipped with special outlets for charging stations. A survey by the US department of energy reported that the average installation costs for level 2 chargers is $3000 [26]. Hence, the installation cost is assumed in this study to be $3,000 per charger. The price for a single pedestal charger is in the range of $400 (wall mount) up to $6,000 [26]. According to the current price of AeroVironment chargers, the cost of chargers is assumed in this work to be $1,870 and $3,275 for single and dual pedestal level 2, 30A chargers, respectively [27]. Based on the listed prices, this work considers only dual pedestal chargers for charging PEVs. The PEV battery rating is normally in the range of 24-65 kWh. The PEV charging price is assumed to be flat at 0.04 $/kWh in addition to the normal price of energy. This work considers both commercial parking lots and residential parking lots of multi-storey building. Moreover, the percentage of commercial charging stations to residential charging stations is maintained at 60 % and 40 %, respectively. As such, 60 % of the PEVs follow commercial parking lots pattern, while 40 % of the PEVs follow residential parking lots pattern.

In this case study, without loss of generality, a PV based RES is considered. The capital cost of the PV system is 3,500 $/kW [28] and the lifetime is 20 years. The step size of the installation is assumed to be 5 kW. Similarly, without loss of generality, LA batteries, as one of the most cost effective DESS technologies, are used in this case study. The parameters of LA batteries are given in Table 2 [28]. It is worth noting that candidate PV and DESS bus locations are typically determined based on a detailed techno-economic planning analysis, which is outside the scope of the presented work and thus assumed to be inputs to this study. For this reason, all the system buses are assumed to be candidate for PV and DESS installations. In order to reduce the computation time, nine locations i.e., 29-38 have been chosen as arbitrary candidates for the PEV charging stations. As shown in Fig.6, the chosen locations are distributed along the test system to cover different areas.

Table 3 shows a description of a number of case studies were conducted as a means of evaluating the merits of the proposed resource allocation framework. Table 4 shows the detailed simulation results of the cost of consumed energy and losses, the expenses of installations for PEVs, PVs, and DESSs, and the profits achieved for the installations in each case study. Table 5 presents the optimal number, sizes and locations of the installed PEVs chargers, PVs, and DESS for each case study. A detailed analysis of the obtained results for each case study is given hereunder.

As shown in Table 4, the total ACOE purchased from the grid in the base case (A), where no allocation is performed, is $1.320M. This energy is the sum of the energy consumed by normal load customers and the energy dissipated as losses with contributions of 97.4 % and 2.6 % respectively. In case A, the overall price of energy was calculated to be 7.02 ¢/kWh, as shown in Table 5.

In case *B*, where only the allocation of PV is considered, it is assumed that the generated energy is sold to the grid at a fixed rate, which represents the incentives from the government to reduce the greenhouse gas emissions. The allocated capacity varies according to the tariff at which the generated energy is sold. Fig.7 shows the cost saving of energy losses and the net profit at different tariff of selling PV when the capital cost of PV installation is $3,500/kW. As shown in the figure, the net profit of installing PV in the system is negative up to around 14.1 ¢/kWh. However, for a tariff above 12.5 ¢/kWh, the sum of the savings in the cost of energy

losses and the net profit is positive; thus, the resource allocation algorithm starts allocating PV units in the system although the cost of installation is higher than the profit of selling energy to the grid.

Fig.8 shows the impact of the tariff of selling PV generation on the optimal installed capacity of PV at different capital costs. As depicted in the figure, the breakeven tariff of selling PV generation increases with the increase of the PV capital costs. For instance, if the capital cost of 1 kW of PV is $2,500/kW, the breakeven tariff is required to be 8 ₡/kWh so that the PV installation investment is economically feasible. While as depicted previously in Fig. 7, when the capital cost is $3,500/kW, the breakeven price is found to be 12.5 ₡/kWh. As depicted in Fig.8, at fixed capital cost of PV installation, the capacity of installed PV increases with the increase of the tariff of selling the PV energy. Due to network constraints, the maximum capacity of PV that can be installed in the grid is found to be 4,000 KW.

In this work, the Feed-in-Tariff (FIT) program in Ontario, Canada, is used as a reference for a 27.5 ₡/kWh [29]. Hence, the total allocated capacity in this case is 4,000 KW, which represents the maximum allowable allocated capacity of PV units in the system. The allocation causes 30.4 % reduction in the annual energy losses and 53.8 % reduction in the cost of energy losses. This is due to the reduction of the losses in periods of high prices. As depicted in Table 4, the annual profit of selling energy to the grid is 90.8 % higher than the annualized installation cost of the PV. Further, the net expenses to operate the system are 72 % lower than the base case and the overall price of energy is 1.96 ₡/kWh, as shown in Table 5.

In case C, the allocation of the DESS without PV installations resulted in a saving of 20.9 % in the cost of energy losses, and an annual profit of $51,457 due to price differences of energy from peak to off-peak periods. The allocated DESS is at bus 31 with a capacity of 200 kW and 875 kWh. The net expenses to run the system are 1.6 % lower than the base case.

Case *D* considers allocating both PV and DESS. The total allocated capacity of PV units in the system is found to be 3,165 kW. On the other hand, one DESS unit is allocated at bus 38 with a total capacity of 625 kW and 3500 kWh. The reduction in the cost of energy loss is 77.8 %, which is very high due to smart scheduling of the charging/discharging of the DESS unit. Compared to the base case scenario, the net expenses are 75.9

% lower. Also, compared with scenario C, the installation of PV units facilitates more capacities for DESS to be installed.

For the PEV stations allocation in case *E*, since it is extra load, the resource allocation algorithm allocates these stations if the profit is higher than the sum of the cost of installation and the increase in the energy losses. The maximum allowable PEV charging stations in the system are 2.5 MW, which represents 285 chargers of level 2. The price of charging PEVs is assumed to be the base energy price plus a fixed profit to cover the capital costs, operating costs, and cost of increased energy loss. For a fixed profit up to 3.25 ¢/kWh, the resource allocation algorithm doesn't allocate any PEV chargers. For a fixed profit of 4 ¢/kWh, however, the resource allocation algorithm allocated 285 chargers. As such, as shown in Table 4, the cost of energy purchased from the grid and consumed by the customers is increased by 14.96 % and the energy loss is increased by 20.9 %. The total expenses to run the system in case E are found to be 2.6 % lower than the base case scenario.

The installation of PV units in case F is allowed to support PEV charging stations. As shown in Table 4, a total capacity of 4,000 kW of PV is installed in the system, which reduces the cost of energy loss by 48.8 % compared to case *E*, and 35.3 % compared to the base case scenario. Also, the net expenses are 74.7 % less than the base case. In case *G*, the algorithm allocates DESS to support the PEV charging stations. As shown in Table 5, 3,000 kW and 5,000 kWh DESS are allocated. Although the allocated capacities are higher than those in cases C and D, the cost of energy loss is still 18.8 % higher than the base case, but 1.8 % lower than case *E*. It is also noted that the net expenses in case G are 18.1 % lower than the base case.

For case *H*, the PV and DESS installations are allowed to support the PEV charging stations. However, the results show that the resource allocation algorithm allocates only PV units in the system without any DESS (i.e.it gives the same results as case *F*). The obtained results are due to: 1) the fact that the PV generation pattern fits PEV charging pattern in commercial lots, while residential PEV charging patterns can easily be shifted to low normal demand period at night, which does not need support from DESS units, and 2) the

incentives from governments for clean energy from PV give superiority for PV allocation in the system compared with much lower profit for allocating DESS units.

6. Conclusion

This paper presents a combined resource allocation framework to accommodate PEV charging load along with RES and DESS in distribution networks. The resource allocation method utilizes a unified scenario based probabilistic approach to optimally allocate PEV charging stations, RES units and DESS simultaneously in order to maximize the profit of the system operators and private investors. The proposed approach incorporates the coordinated operation scheduling of PEV charging, DESS charging/discharging, and output power control of RES inverters in the resource allocation process. The resource allocation problem is formulated as MINLP, which is decomposed and solved using, a combination between GA and deterministic optimization tools. The presented approach can help LDCs and their stakeholders to optimize their investments. The proposed resource allocation framework has been applied in a sample case study to test its performance. The conclusion drawn from the presented case study is that a significant profit can be achieved by allocating PV units to support PEV charging stations. On the other hand, DESS units do not present significant support for PEV charging stations, either for commercial or residential charging stations. Though the drawn conclusion is a case specific that cannot be generalized, the proposed resource allocation methodology is systematic and generalized. Hence, it can be utilized as a useful tool for LDC planners and their stakeholders to make appropriate decisions for the investment in the combined PEVs charging stations, RES and DESS installations.

7. Acknowledgments

The authors of this article would like to acknowledge support from Natural Sciences and Engineering Research Council of Canada (NSERC) Grant No: RGPIN 1510.

References

[1] M. Noori and O. Tatari, "Development of an agent-based model for regional market penetration projections of electric vehicles in the United States," *Energy*, vol. 96, pp. 215–230, Feb. 2016.

[2] I. Graabak, Q. Wu, L. Warland, and Z. Liu, "Optimal planning of the Nordic transmission system with 100% electric vehicle penetration of passenger cars by 2050," *Energy*, vol. 107, pp. 648–660, Jul. 2016.

[3] E. Ramos Muñoz, G. Razeghi, L. Zhang, and F. Jabbari, "Electric vehicle charging algorithms for coordination of the grid and distribution transformer levels," *Energy*, vol. 113, pp. 930–942, Oct. 2016.

[4] A. Kavousi-Fard, A. Abbasi, M.-A. Rostami, and A. Khosravi, "Optimal distribution feeder reconfiguration for increasing the penetration of plug-in electric vehicles and minimizing network costs," *Energy*, vol. 93, Part 2, pp. 1693–1703, Dec. 2015.

[5] J. Hu, H. Morais, T. Sousa, and M. Lind, "Electric vehicle fleet management in smart grids: A review of services, optimization and control aspects," *Renew. Sustain. Energy Rev.*, vol. 56, pp. 1207–1226, Apr. 2016.

[6] H. Fathabadi, "Utilization of electric vehicles and renewable energy sources used as distributed generators for improving characteristics of electric power distribution systems," *Energy*, vol. 90, Part 1, pp. 1100–1110, Oct. 2015.

[7] S. Shokrzadeh and E. Bibeau, "Sustainable integration of intermittent renewable energy and electrified light-duty transportation through repurposing batteries of plug-in electric vehicles," *Energy*, vol. 106, pp. 701–711, Jul. 2016.

[8] S. F. Abdelsamad, W. G. Morsi, and T. S. Sidhu, "Impact of Wind-Based Distributed Generation on Electric Energy in Distribution Systems Embedded With Electric Vehicles," *IEEE Trans. Sustain. Energy*, vol. 6, no. 1, pp. 79–87, Jan. 2015.

[9] S. Vazquez, S. M. Lukic, E. Galvan, L. G. Franquelo, and J. M. Carrasco, "Energy Storage Systems for Transport and Grid Applications," *IEEE Trans. Ind. Electron.*, vol. 57, no. 12, pp. 3881–3895, Dec. 2010.

[10] L. W. Chong, Y. W. Wong, R. K. Rajkumar, R. K. Rajkumar, and D. Isa, "Hybrid energy storage systems and control strategies for stand-alone renewable energy power systems," *Renew. Sustain. Energy Rev.*, vol. 66, pp. 174–189, Dec. 2016.

[11] R. Hemmati and H. Saboori, "Emergence of hybrid energy storage systems in renewable energy and transport applications – A review," *Renew. Sustain. Energy Rev.*, vol. 65, pp. 11–23, Nov. 2016.

[12] C. Jin, J. Tang, and P. Ghosh, "Optimizing Electric Vehicle Charging With Energy Storage in the Electricity Market," *IEEE Trans. Smart Grid*, vol. 4, no. 1, pp. 311–320, Mar. 2013.

[13] L. Liu, F. Kong, X. Liu, Y. Peng, and Q. Wang, "A review on electric vehicles interacting with renewable energy in smart grid," *Renew. Sustain. Energy Rev.*, vol. 51, pp. 648–661, Nov. 2015.

[14] H. Kamankesh, V. G. Agelidis, and A. Kavousi-Fard, "Optimal scheduling of renewable micro-grids considering plug-in hybrid electric vehicle charging demand," *Energy*, vol. 100, pp. 285–297, Apr. 2016.

[15] G. Haddadian, N. Khalili, M. Khodayar, and M. Shahidehpour, "Optimal coordination of variable renewable resources and electric vehicles as distributed storage for energy sustainability," *Sustain. Energy Grids Netw.*, vol. 6, pp. 14–24, Jun. 2016.

[16] W. Hu, C. Su, Z. Chen, and B. Bak-Jensen, "Optimal Operation of Plug-In Electric Vehicles in Power Systems With High Wind Power Penetrations," *IEEE Trans. Sustain. Energy*, vol. 4, no. 3, pp. 577–585, Jul. 2013.

[17] S. Gao, K. T. Chau, C. Liu, D. Wu, and C. C. Chan, "Integrated Energy Management of Plug-in Electric Vehicles in Power Grid With Renewables," *IEEE Trans. Veh. Technol.*, vol. 63, no. 7, pp. 3019–3027, Sep. 2014.

[18] A. El-Zonkoly, H. Ashour, and A. Ahmed, "Optimal allocation, sizing and energy management of PHEV parking lots in distribution system," in *Renewable Energy Congress (IREC), 2014 5th International*, 2014, pp. 1–5.

[19] N. Neyestani, M. Y. Damavandi, M. Shafie-khah, J. P. S. Catalão, and J. Contreras, "Allocation of PEVs' Parking lots in renewable-based distribution system," in *Power Engineering Conference (AUPEC), 2014 Australasian Universities*, 2014, pp. 1–6.

[20] M. F. Shaaban, Y. M. Atwa, and E. F. El-Saadany, "PEVs modeling and impacts mitigation in distribution networks," *IEEE Trans. Power Syst.*, vol. 28, no. 2, pp. 1122–1131, May 2013.

[21] M. F. Shaaban and E. F. El-Saadany, "Accommodating High Penetrations of PEVs and Renewable DG Considering Uncertainties in Distribution Systems," *IEEE Trans. Power Syst.*, vol. 29, no. 1, pp. 259–270, Jan. 2014.

[22] Z. Liu, D. Wang, H. Jia, N. Djilali, and W. Zhang, "Aggregation and Bidirectional Charging Power Control of Plug-in Hybrid Electric Vehicles: Generation System Adequacy Analysis," *IEEE Trans. Sustain. Energy*, vol. 6, no. 2, pp. 325–335, Apr. 2015.

[23] M. Moeini, H. Farzin, M. Fotuhi-Firuzabad, and R. Amrollahi, "Generalized Analytical Approach to Assess Reliability of Renewable-Based Energy Hubs," *IEEE Trans. Power Syst.*, vol. PP, no. 99, pp. 1–1, 2016.

[24] H. Farzin, M. Fotuhi-Firuzabad, and M. Moeini, "Reliability Studies of Modern Distribution Systems Integrated With Renewable Generation and Parking Lots," *IEEE Trans. Sustain. Energy*, vol. PP, no. 99, pp. 1–1, 2016.

[25] Josh Agenbroad, Ben Holland, Pulling Back the Veil on EV Charging Station Costs, http://blog.rmi.org/

[26] M. Smith, " Non-Residential Electric Vehicle Supply Equipment Costs." US department of energy, Los Angeles, CA, USA (2012).

[27] The Home Depot [Online]. Available: homedepot.com, accessed January 2017

[28] C. H. Lin, W. L. Hsieh, C. S. Chen, C. T. Hsu, and T. T. Ku, "Optimization of Photovoltaic Penetration in Distribution Systems Considering Annual Duration Curve of Solar Irradiation," *IEEE Trans. Power Syst.*, vol. 27, no. 2, pp. 1090–1097, May 2012.

[29] "FIT Price Schedule | Feed-in Tariff Program - Independent Electricity System Operator." [Online]. Available: http://fit.powerauthority.on.ca/fit-program/fit-program-pricing/fit-price-schedule.

Figures Caption:

Fig.1: Proposed framework for integration of operation scheduling in resource allocation studies

Fig.2: Proposed scenario-based PEV arrival rate model

Fig.3: Sample of generated scenarios of PEVs arrival rate profiles

Fig.4: Four-quadrant model of DESS inverters

Fig.5: Proposed resource allocation algorithm structure

Fig.6: The 38-bus distribution test system

Fig.7: Impact of the tariff of selling PV energy on the cost saving of energy losses and the net profit

Fig.8: Impact of tariff of selling PV generation on the total installed PV capacity at different capital costs of PV installation

Tables Caption:

Table 1: Data of PEVs and charging station

Table 2: Data of LA battery [28]

Table 3: Description of the conducted case studies

Table 4: Cost related results

Table 5: Optimal resource allocations and cost of energy in $/KWh

Table 1

PEV batteries capacities	24 – 65 kWh
Charging cost	0.04 $/kWh + Energy price
PEV charger ratings	208-240Volt AC, 7.2kW, 30Amp
Price for single pedestal charger	$1,870 (AeroVironment)
Price for dual pedestal charger	$3,275 (AeroVironment)
Cost of labour, permits, and material	$3,000/charger
Percentage of commercial charging stations	60 %
Percentage of residential charging stations	40 %

Table 2

Power capital cost	175 $/kW
Energy capital cost	305 $/kWh
Annual operation and maintenance cost	15 $/kW
Round-trip efficiency	75%
Life-time	3200 cycles
Maximum battery size	1000 kW – 1000 kWh
$P_{BES-kW}^{Step}, P_{BES-kWh}^{Step}$	25 kW, 25 kWh

Table 3

Case	Description	Case	Description
A	Base case	***B***	PV allocation
C	DESS allocation	***D***	PV and DESS allocation
E	PEV stations allocation	***F***	PEV stations and PV allocation
G	PEV stations and DESS allocation	***H***	PEV stations, PV and DESS allocation

Table 4

Case		*A* *Base Case*	*B* *PV*	*C* *DESS*	*D* *PV+DESS*	*E* *EV*	*F* *PV+EV*	*G* *DESS+EV*	*H* *PV+DESS+EV*
CONSUMED ENERGY	**($)**	1,286,360	1,286,360	1,286,360	1,286,360	1,467,436	1,478,122	1,600,843	1,478,122
	(%)*	0.00%	0.00%	0.00%	0.00%	14.08%	14.91%	24.45%	14.91%
Energy LOSS	**($)**	33,880	15,655	26,800	7,511	40,980	21,914	40,250	21,914
	(%)*	0.00%	-53.79%	-20.90%	-77.83%	20.96%	-35.32%	18.80%	-35.32%
EXPENSES ($)	**RES**	0	1,026,543		1,026,543	0	1,026,543	0	1,026,543
	DESS	0	0	37,519	143,397	0	0	257,683	0
PROFIT ($)	**EV chargers**	0	0	0	0	162,092	162,092	162,092	162,092
	RES	0	1,959,130	0	1,959,130	0	1,959,130	0	1,959,130
	DESS	0	0	51,457	187,252	0	0	461,441	0
	EV chargers	0	0	0	0	384,315	395,001	517,722	395,001
NET	**($)**	1,320,240	369,428	1,299,222	317,429	1,286,193	333,587	1,081,705	333,587
	(%)*	0.00%	-72.02%	-1.59%	-75.96%	-2.58%	-74.73%	-18.07%	-74.73%

*Percentage increase from base case

Table 5

Case		*A* *Base Case*	*B* *PV*	*C* *DESS*	*D* *PV+DESS*	*E* *EV*	*F* *PV+EV*	*G* *DESS+EV*	*H* *PV+DESS+EV*
LOSSES	**(MWh)**	427	297	663	459	738	369	1042	369
	(%)*	0.00%	-30.44%	55.27%	7.49%	72.83%	-13.58%	144.03%	-13.58%
RES ALLOCATION	**Bus**	–	5, 6, 8, 9, 10, 11, 12, 13, 14, 15, 16, 17, 18, 21, 22, 24, 25, 26, 27, 28, 29, 30, 31, 32, 33, 34, 37	–	4, 5, 6, 7, 10, 11, 12, 13, 16, 17, 18, 20, 23, 24, 25, 26, 29, 30, 31, 32, 38	–	6, 7, 8, 9, 10, 11, 12, 13, 14, 15, 16, 17, 18, 22, 24, 25, 26, 27, 28, 29, 30, 31, 32, 33, 34, 38	–	6, 7, 8, 9, 10, 11, 12, 13, 14, 15, 16, 17, 18, 22, 24, 25, 26, 27, 28, 29, 30, 31, 32, 33, 34, 38
	(kW)	–	5, 150, 125, 30, 75, 115, 190, 190, 275, 120, 180, 130, 155, 15, 35, 160, 335, 30, 20, 30, 110, 600, 275, 545, 85, 5, 15	–	90, 20, 215, 25, 75, 80, 165, 160, 125, 120, 130, 50, 25, 565, 505, 55, 125, 505, 60, 50, 30	–	115, 20, 100, 15, 60, 80, 80, 120, 200, 100, 105, 100, 150, 25, 130, 225, 30, 15, 30, 610, 560, 185, 390, 85, 395, 75	–	115, 20, 100, 15, 60, 80, 80, 120, 200, 100, 105, 100, 150, 25, 130, 225, 30, 15, 30, 610, 560, 185, 390, 85, 395, 75
	Total (kW)	–	4000	–	3175	–	4000	–	4000
DESS ALLOCATION	**Bus**	–	–	31	38	–	–	35	–
	(kW)	–	–	200	625	–	–	3000	–
	(kWh)	–	–	875	3500	–	–	5000	–
PEV CHARGES ALLOCATION	**Bus**	–	–	–	–	29, 34, 35, 38	29,34,35,38	29,33,34,38	29,34,35,38
	Number	–	–	–	–	60, 100, 28, 100	60,100,28,100	98,10,76,100	60,100,28,100
COST OF ENERGY	**($/kWh)**	0.0702	0.0196	0.0691	0.0169	0.0321	0.0096	0.0405	0.0096

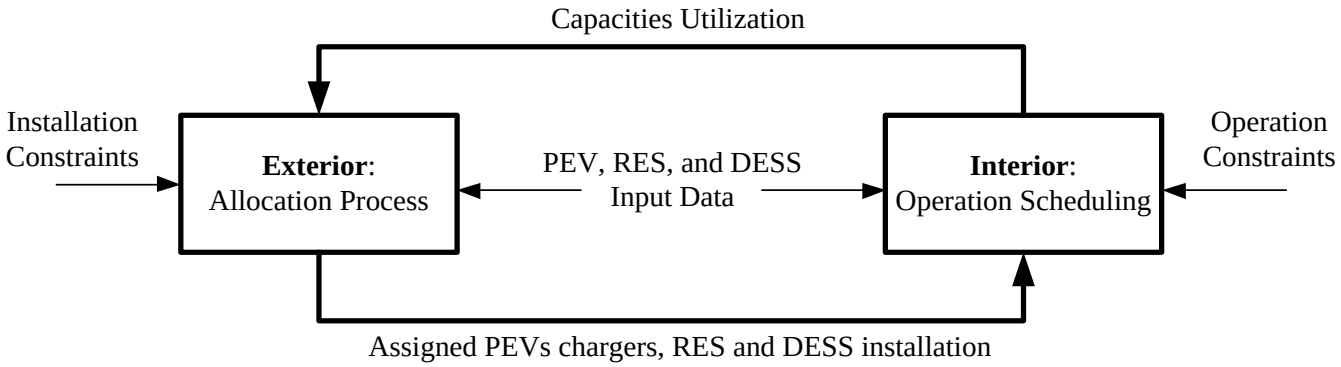
Capacities Utilization
Installation Constraints
Exterior: Allocation Process
PEV, RES, and DESS Input Data
Interior: Operation Scheduling
Operation Constraints
Assigned PEVs chargers, RES and DESS installation

Fig.1

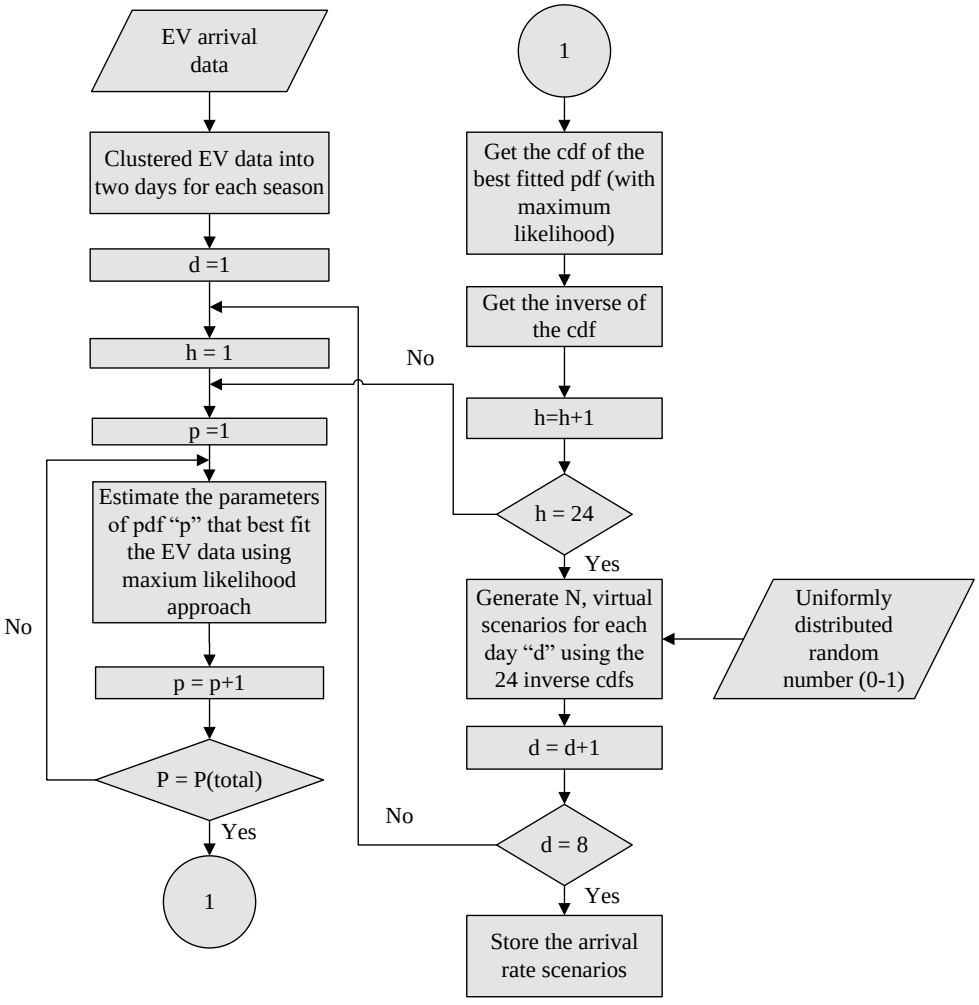
EV arrival data
Clustered EV data into two days for each season
d =1
h = 1
p =1
Estimate the parameters of pdf "p" that best fit the EV data using maxium likelihood approach
p = p+1
P = P(total)
No
Yes
1
1
Get the cdf of the best fitted pdf (with maximum likelihood)
Get the inverse of the cdf
h=h+1
h = 24
No
Yes
Generate N, virtual scenarios for each day "d" using the 24 inverse cdfs
Uniformly distributed random number (0-1)
d = d+1
d = 8
No
Yes
Store the arrival rate scenarios

Fig.2

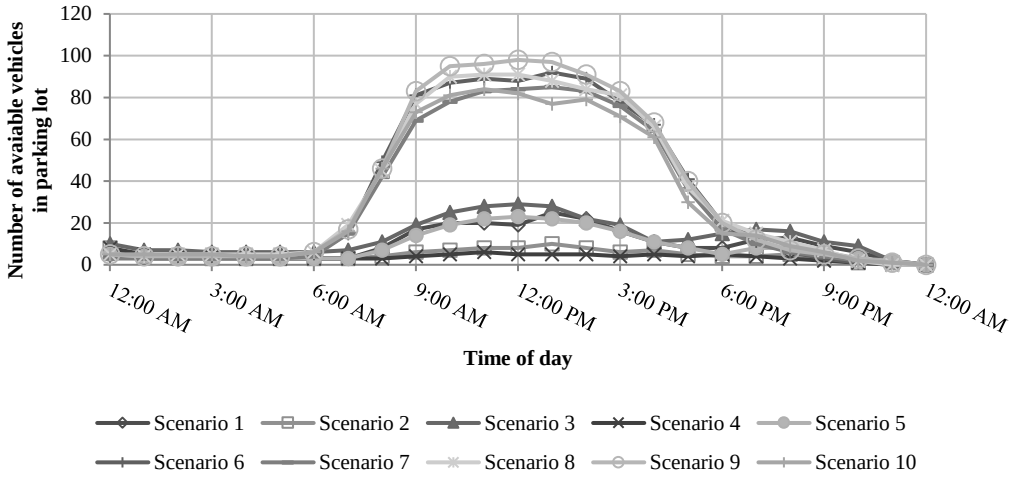
Number of avaiable vehicles in parking lot
120
100
80
60
40
20
0
12:00 AM
3:00 AM
6:00 AM
9:00 AM
12:00 PM
3:00 PM
6:00 PM
9:00 PM
12:00 AM
Time of day
Scenario 1
Scenario 2
Scenario 3
Scenario 4
Scenario 5
Scenario 6
Scenario 7
Scenario 8
Scenario 9
Scenario 10

Fig.3

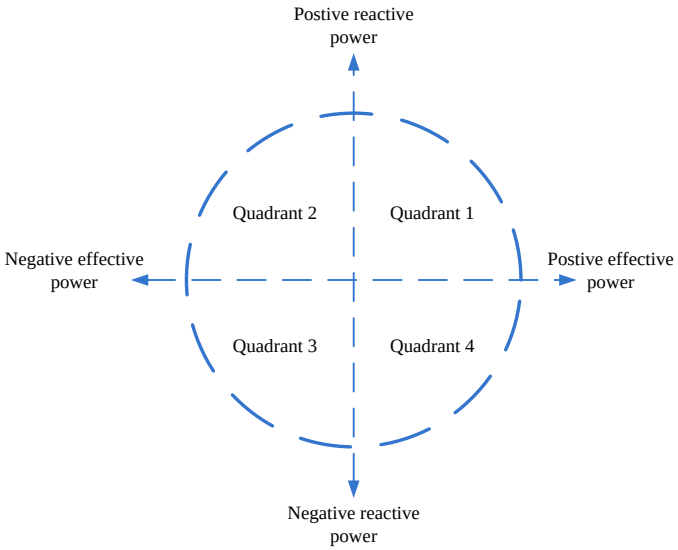
Postive reactive power
Quadrant 2
Quadrant 1
Negative effective power
Postive effective power
Quadrant 3
Quadrant 4
Negative reactive power

Fig.4

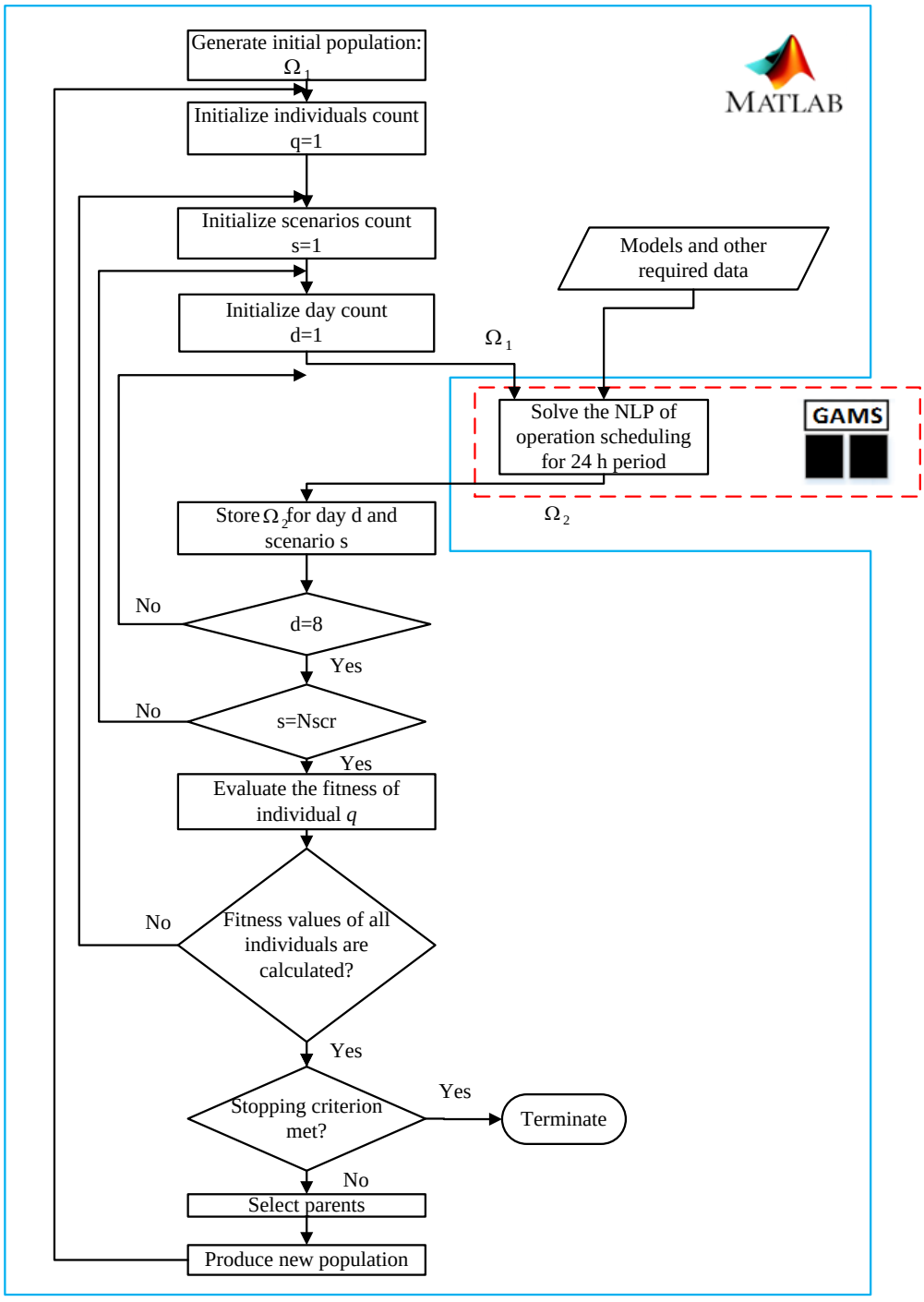
Generate initial population: Ω1
Initialize individuals count q=1
Initialize scenarios count s=1
Initialize day count d=1
Models and other required data
Ω1
Solve the NLP of operation scheduling for 24 h period
GAMS
Store Ω2 for day d and scenario s
Ω2
No
d=8
Yes
No
s=Nscr
Yes
Evaluate the fitness of individual q
No
Fitness values of all individuals are calculated?
Yes
Yes
Stopping criterion met?
Terminate
No
Select parents
Produce new population
MATLAB

Fig.5

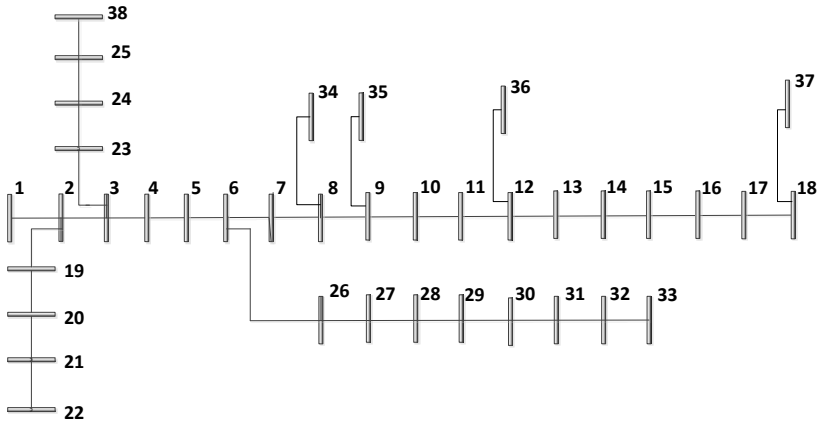

Fig.6

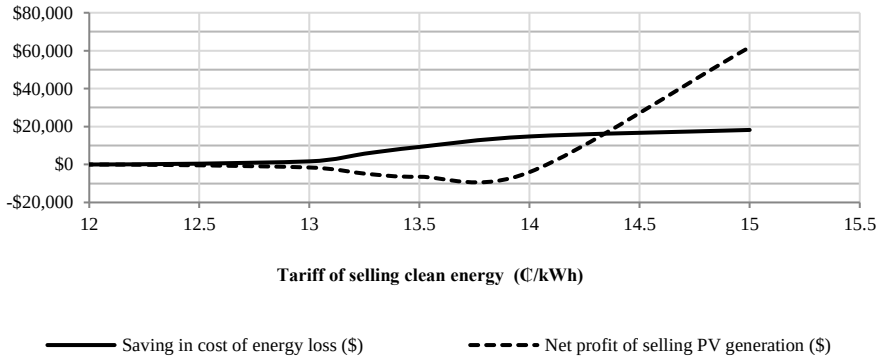

Fig.7

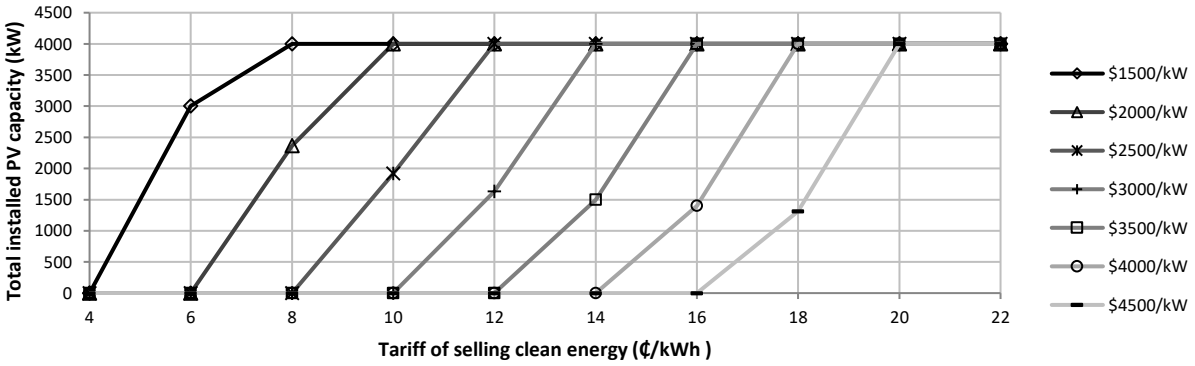

Fig.8